Toward Generation of Orbital-Angular-Momentum-Entangled Photon Pairs in a Few-Mode Fiber

Afshin Shamsshooli, Cheng Guo, Francesca Parmigiani, Xiaoying Li, and Michael Vasilyev 1*

¹Department of Electrical Engineering, University of Texas at Arlington, Arlington, TX 76019, USA

²Microsoft Research, Cambridge, CB1 2FB, UK

³College of Precision Instruments and Opto-electronics Engineering, Key Laboratory of Opto-electronic Information Technical Science of

Ministry of Education, Tianjin University, Tianjin, 300072, China *E-mail: vasilyev@uta.edu

Abstract: We describe a novel scheme for generation of orbital-angular-momentum-entangled photons in a few-mode fiber. We experimentally verify the underlying inter-modal parametric processes with two-mode classical signal input, observing high mode purity of the generated idler. **OCIS codes:** (190.4380) Nonlinear optics, four-wave mixing; (190.4420) Nonlinear optics, transverse effects in; (060.4370) Nonlinear optics, fibers; (270.5585) Quantum information and processing.

The use of spatial modes (e.g., those of multimode fibers and waveguides) is important for increasing capacity of both classical and quantum communications. In the quantum case, entanglement in multiple degrees of freedom (e.g., in polarization, frequency, time-bin, and spatial modes) may enable new communication and networking protocols relying on quantum information encoding in high-dimensional Hilbert space. While polarization, frequency, and time-bin entanglement generation has already been implemented in integrated form compatible with low-loss transport over optical fiber, the spatial entanglement still relies on bulk-crystal-based setups, e.g., spatially- or orbital-angular-momentum- (OAM) entangled photons have been generated in crystal platforms and transported over hollow-core photonic crystal fiber [1], a few-mode fiber (FMF) [2], and vortex fiber [3]. FMF itself has been gaining traction as a nonlinear platform based on inter-modal four-wave mixing (IM-FWM), owing to FMF's wide options for mode- and dispersion-engineering, and excellent mode match to the FMFs used in low-loss transmission links. Correlated photon pairs were recently generated in FMFs by IM-FWM [4, 5], but no attempts of spatial-mode entanglement have been made yet. We have recently described a novel scheme for generation of spatial-mode-entangled photon pairs in LP₀₁ and LP₁₁ modes directly in the FMF using a combination of two IM-FWM processes [6]. Using classical seed signals, we experimental demonstrated signal-idler mode selectivity separately for these two processes. In this paper, we show how a modification of that scheme can be used to generate orbital-angular-momentum-entangled photon pairs.

Our spatial-mode entanglement scheme employs a combination of two IM-FWM processes of Fig. 1a. We use an elliptical-core FMF [7], to be referred to as three-mode fiber (TMF) below, which supports three non-degenerate modes: LP₀₁, LP_{11a}, and LP_{11b}. In IM-FWM process 1, with the help of pumps 1 and 2 a signal photon is created in mode LP_{11a} at frequency v_s , while idler photon is created in mode LP_{11b} at frequency v_i . In process 2, their roles interchange: in the presence of pumps 3 and 4, signal photon at frequency v_s is created in mode LP_{11b}, whereas the idler photon at frequency v_i is created in mode LP_{11a}. With all four pumps present, processes 1 and 2 take place simultaneously. Their probabilities can be equalized by adjusting relative powers of the two pump pairs, which results in generation of the maximally-entangled state $|LP_{11b}\rangle_s|LP_{11a}\rangle_i + e^{i\phi}|LP_{11a}\rangle_s|LP_{11b}\rangle_i$, where phase ϕ can be changed by varying the pump phase difference $\Delta \varphi = (\varphi_{p1} + \varphi_{p2}) - (\varphi_{p3} + \varphi_{p4})$. For $\varphi = \pi$ this state is equivalent to the OAMentangled state $|l = +1\rangle_s |l = -1\rangle_i - |l = -1\rangle_s |l = +1\rangle_i$, where l is the orbital quantum number. For each of the two processes in Fig. 1a, the phase-matching condition [8] requires equal group velocities at the average frequencies of the two waves present in each spatial mode. These average frequencies, converted to wavelengths, are shown by dashed lines in Fig. 1a. Figure 1b shows measured relative inverse group velocities (RIGV) 1/v_e of LP₀₁, LP_{11a}, and LP_{11b} modes of our TMF. The LP_{11b} curve is approximately parallel to the LP_{11a} curve and horizontally shifted from it by ~ 17 nm ($\Delta v_1 = 2.1$ THz), i.e., the phase matching is satisfied when the dashed lines in Fig. 1a are separated by 17 nm. Energy conservation and momentum conservation (phase matching) impose 4 constraints on the frequencies of the 6 involved waves: $v_{p1(p3)} = v_{i(s)} + \Delta v_1$ and $v_{p2(p4)} = v_{s(i)} - \Delta v_1$, hence any two frequencies that are not separated by Δv_1 can be arbitrarily chosen. In our experiment, we choose signal to be at 1564.8 nm and idler to be at 1558.4 nm, which results in pumps 1, 2, 3, and 4 placed at 1541.3, 1582.4, 1547.3, and 1576.1, respectively.

Our experimental setup is shown in Fig. 1c. The test signal and pumps are carved into 10-ns-long flat-top pulses with a 10-MHz repetition rate by intensity modulators and are amplified by telecom-grade C- and L-band erbium-doped fiber amplifiers (EDFAs). In process 1, signal and pump 1 are collimated and combined by a beam splitter BS in free-space. Their spatial modes are individually converted to LP_{11a} by two corresponding phase plates PP1 and PP2. Pump 2 is collimated into free space, converted to LP_{11b} mode by a phase plate PP3, and combined with signal and pump 1 via a dichroic beam splitter DBS. The three waves are then coupled into a 1-km-long TMF by an objective. The TMF output is collimated by a second objective. Part of the output is observed on an infrared camera, and the remainder is coupled into a single-mode fiber (SMF) connected to the optical spectrum analyzer (OSA), which in this

case measures the LP_{01} "output port" of the TMF. By inserting phase plate PP4 prior to SMF coupling, we can also measure LP_{11a} and LP_{11b} "output ports" of the TMF. In process 2, pump 1 and pump 2 are replaced by pump 3 and pump 4, respectively, by an optical switch (OS). For this process, signal is changed to LP_{11b} mode by PP1. In future experiments, the OS will be replaced by wavelength multiplexers to enable simultaneous presence of all 4 pumps. To maximize IM-FWM, we co-polarize all three input waves entering the TMF. We characterize idler-mode impurity by comparing idlers in LP_{11a} and LP_{11b} output ports of the TMF. The depth of suppression of undesirable parametric interactions, i.e., mode selectivity of the parametric amplification processes 1 and 2, is quantified by comparing the idler generated by the desired process to that generated by an undesirable process, observed when the input signal is injected into a wrong mode: LP_{11b} for process 1, LP_{11a} for process 2.

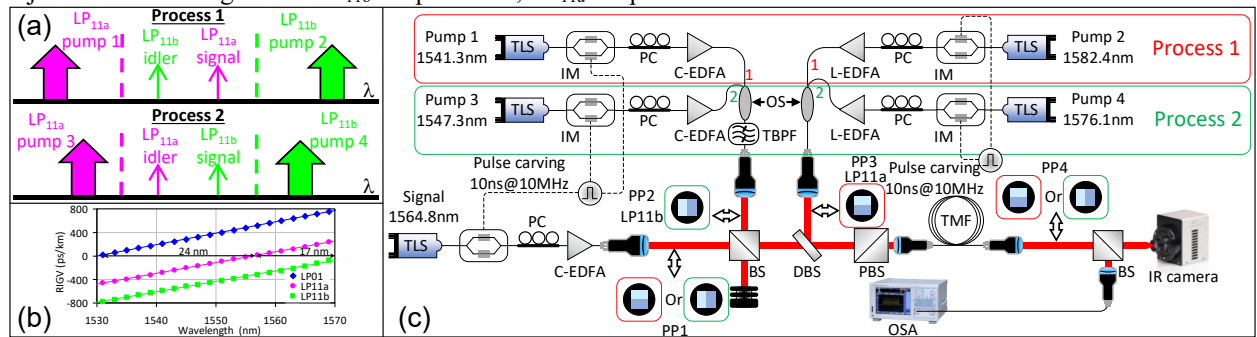


Fig.1. (a) Two parametric processes, whose combination enables generation of orbital-angular-momentum-entangled signal-idler photon pairs in the TMF. (b) Measured relative inverse group velocity (RIGV) data for the modes of our TMF. (c) Experimental setup.

Figure 2 shows the spectra at the LP_{11a} (blue traces) and LP_{11b} (magenta traces) output ports of the TMF for processes (a) 1 and (b) 2. One can easily see a significant change in the idler power between the two traces, indicating high spatial-mode purity of the idler (18.1 and 18.7 dB for processes 1 and 2, respectively). Average powers inside the TMF are 0 dBm for the signal in all cases and 15, 9.5, 17, and 7.5 dBm for pumps 1, 2, 3, and 4, respectively. Easily-measurable signal-to-idler conversion efficiency is given by $CE = g - 1 = \langle n \rangle$, where g is the phase-insensitive parametric gain, and $\langle n \rangle$ is the average number of generated parametric photons per mode, also representing the probability of a single pair generation for our case of $CE \ll 1$. In Fig. 2, CEs are -46.1 and -47.1 dB for processes 1 and 2, respectively. The CEs of the undesirable processes, measured by injecting the signal into the wrong mode, are suppressed by more than 20 and 18.4 dB, compared to processes 1 and 2, respectively (not shown in Fig. 2).

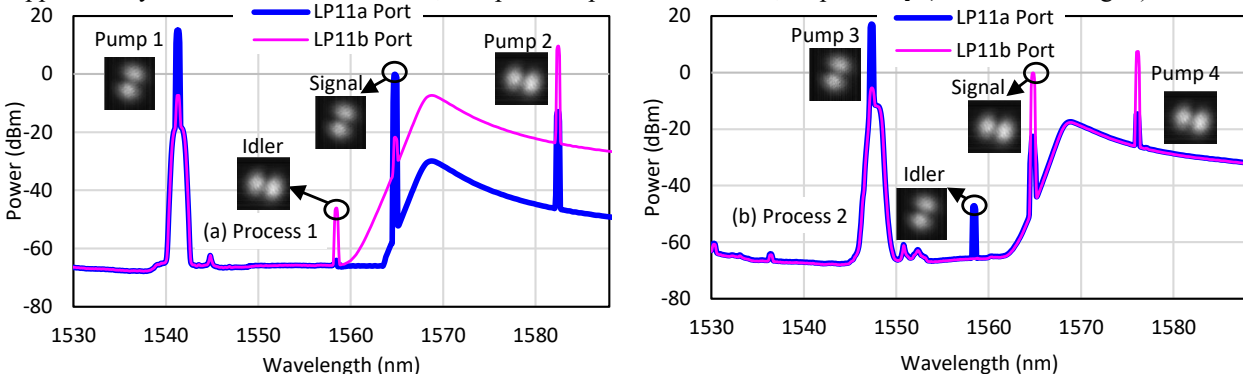


Fig. 2. Optical spectra, measured at the LP_{11a} (blue traces) and LP_{11b} (magenta traces) output ports of the TMF for processes (a) 1 (signal in LP_{11a} mode) and (b) 2 (signal in LP_{11b} mode).

To summarize, we used classical signal to experimentally verify mode-selective properties of the novel scheme for generation of OAM-entangled photons, in which low-gain parametric amplifier in TMF couples LP_{11a} signal to LP_{11b} idler and LP_{11b} signal to LP_{11a} idler. In the spontaneous regime, the combination of these two processes would generate OAM-entangled signal-idler photon pairs. The next step is to optimize the pump multiplexing scheme, both to minimize the losses and to reduce the fluctuations of pump phase difference $\Delta \phi$. Spontaneous regime would, in addition, require strong suppression of the amplified spontaneous emission of the pump beams at signal and idler frequencies, as well as narrow bandpass filtering of the output to minimize contribution of Raman noise [9].

This work has been supported in part by the NSF grants ECCS-1937860 and ECCS-1842680.

References

- [1] W. Löffler et al, PRL 106, 240505 (2011). [4] K. Rottwitt et al, Fibers 6, 32 (2018). [7] F. Parmigiani et al, OE 25, 33602 (2017).
- [2] Y. Kang et al, PRL 109, 020502 (2012). [5] C. Guo et al, Opt Lett 44, 235 (2019). [8] R.-J. Essiambre et al, PTL 25, 539 (2013).
- [3] D. Cozzolino etal, Adv Phot 1, 046005 (2019). [6] A. Shamsshooli et al, CLEO 2020, JTh2A.29. [9] Y. B. Kwon et al, CLEO 2017, FF2E.1.